# Dynamical Response and Firing Patterns in Periodically Pulsed Bromate−Sulfite−Ferrocyanide System

**Oldřich Pešek, Pavel Kašpar, Lenka Schreiberová, and Igor Schreiber***

*Department of Chemical Engineering & Center for Nonlinear Dynamics of Chemical and Biological Systems, Prague Institute of Chemical Technology, Technická 5, 16628 Prague 6, Czech Republic*

*Received: July 17, 2003; In Final Form: November 26, 2003*

Bromate-sulfite-ferrocyanide reaction operated in the CSTR is sensitive to small but supercritical additions of either acid or base. When operated at two different kinds of steady states, this dynamical feature gives rise to activatory or inhibitory excitability. Spontaneous periodic oscillations are also sensitive to such perturbations. Periodically repeated pulse additions elicit a pattern of excitatory or oscillatory spikes that depends on the period and amplitude of the perturbations. These firing patterns are characterized by firing number defined as an average number of firings per a forcing period. Experiments with periodically pulsed additions of $H^+$, $OH^-$, and $SO_3^{2-}$ provide one-parameter and two-parameter firing diagrams. Recently, a detailed model has been formulated; using this model, we study global dynamics of the response by calculating firing diagrams under conditions corresponding to experiments. The experimental results are compared with calculations.

## 1. Introduction

The response of an excitable system to periodic perturbations in a flow-through reactor has been earlier studied mostly by using the Belousov−Zhabotinskyi (BZ) reaction.[1−5] Other chemical systems displaying oscillations and multiple steady states are also capable of displaying excitability[6−9] because excitability typically occurs in the parameter region between oscillations and bistability. In this paper, we experimentally examine the response dynamics of the bromate−sulfite−ferrocyanide (BSF) system.[10,11] This reaction provides an example of a pH-autocatalytic system therefore perturbations can be conveniently done by adding either acid or base. For systems with a cross-shaped bifurcation diagram,[12,13] excitability may occur in two different modes, *activatory* and *inhibitory* excitability.[6,7,14] In our previous work,[6,7] we have found that this generic behavior is also displayed by the BSF reaction. In the absence of perturbations, the dynamical regime in the CSTR is set to one of two distinct steady states: the acidic steady state (SSA) or the weakly acidic steady state (SSB). The type of the steady state is selected by choosing appropriate residence time in the reactor. Then a perturbant (sulfuric acid, sodium hydroxide, or sodium sulfite) is periodically added via brief injection pulses, and the response of the system is observed. If subject to periodic pulse perturbations, the BSF reaction in the CSTR displays a rich variety of dynamical regimes, including complex periodic and nonperiodic oscillations. These regimes are characterized by firing number. By systematically varying the period of the perturbation and the perturbation size (or amplitude), we obtain one-parameter and two-parameter plots of the firing number: excitation diagrams. The experimental diagrams are compared with those calculated from a recently proposed improved mechanism of the BSF reaction.[7]

## 2. Experimental Section

All of the experiments were carried out in a jacketed CSTR made of Plexiglas and having metal bottom to ensure a rapid heat exchange with the cooling water. The temperature in the reactor was controlled by a thermostat and kept at 40 ± 0.5 °C. The CSTR with a volume of 18.2 mL was stirred magnetically with a frequency of 1500 rpm. The reactor was furnished with five inlet and one outlet streams. A peristaltic pump (Ismatec) delivered reactants through four inlet streams (solutions of $BrO_3^-$, $SO_3^{2-}$, $Fe(CN)_6^{4-}$, and $H_2SO_4$); the fifth one was used for pulsed perturbations made by injecting a solution of a chosen perturbant (NaOH, $H_2SO_4$, or $Na_2SO_3$) delivered by a syringe pump. The reactor was equipped with a platinum resistance thermometer and a glass combined pH-semi-microelectrode (Theta) for monitoring temperature and pH, respectively. The whole process was controlled, and data recorded, by a computer.

Stock solutions were prepared from analytical grade crystalline $NaBrO_3$, $Na_2SO_3$, $K_4Fe(CN)_6{\cdot}3H_2O$, and NaOH and concentrated liquid $H_2SO_4$. Based on our earlier work,[7] we have chosen the following inflow concentrations of the reactants: $c(BrO_3^-) = 0.075$ M, $c(SO_3^{2-}) = 0.07$ M, $c(Fe(CN)_6^{4-}) = 0.015$ M, $c(H_2SO_4) = 7.5 \times 10^{-3}$ M. The used perturbants were 0.1 M NaOH, 1 M $H_2SO_4$, and 0.85 M $Na_2SO_3$ injected into the reactor in a certain (small) volume. The amplitude $\Delta c$ of the perturbation is defined as moles of added perturbant divided by the volume of the reaction mixture; that is, $\Delta c$ is an instantaneous increase in concentration of the perturbant in the reactor caused by the pulse.

Autonomous dynamical regimes were set by adjusting the value of the reciprocal residence time $k_0$ defined as the ratio of the inlet volumetric flow to the reactor volume. In our previous experiments,[6,7] we found that by varying $k_0$ one of the following types of dynamical regimes can be observed: (a) acidic stationary state SSA with pH ≈ 4 ($k_0 < 0.0009$ s$^{-1}$), (b) periodic oscillations (0.0009 s$^{-1}$ < $k_0$ < 0.0031 s$^{-1}$), and (c) weakly acidic stationary state SSB with pH ≈ 6 ($k_0 > 0.031$ s$^{-1}$). The ranges of existence as well as pH traces for these regimes are very well reproduced in the present experiments (including oscillatory periods), even though we use a different type of reactor (with magnetic stirring) than earlier (stirred with a

* To whom correspondence should be addressed. E-mail: schrig@vscht.cz. Telephone: +420 2 2435 3167. Fax: +420 2 3333 7335.

10.1021/jp036086a CCC: $27.50 
Published on Web 03/05/2004

Rushton turbine impeller). These observations and additional test experiments using different stirring rates indicate that stirring effects are insignificant. Based on these results, in the experiments presented here, we chose a value of the reciprocal residence time from each of these ranges and examined the effect of periodic perturbations by using relevant perturbants. The experiments were performed at $k_0 = 8.0 \times 10^{-4}$ s$^{-1}$ for the SSA, at $k_0 = 2.0 \times 10^{-3}$ s$^{-1}$ for the oscillatory regime, and at $k_0 = 3.6 \times 10^{-3}$ s$^{-1}$ for the SSB. Both SSA and SSB were chosen at conditions close to the oscillatory transition because excitability there is well developed. Conditions for the oscillatory regime were chosen approximately in the middle of the oscillatory range, the autonomous period of these oscillations was $T_B = 520$ s. The perturbants were sodium hydroxide and sodium sulfite for SSA, sulfuric acid for SSB, and sodium hydroxide as well as sulfuric acid for periodic oscillations.

### 3. Mechanism and Reduced Mathematical Model

The mechanism presented here (see also refs 6 and 7) is an extension of ref 11 and is based on successive reduction of bromate by protonated forms of sulfite.[15] In addition, we introduce a second reduction pathway for bromate via ferrocyanide and include $BrO_2^-$ as a dynamical intermediate. Thereby, both reduction pathways are allowed to interact, which enables us to obtain a much better fit with the experimentally observed dynamics compared to earlier models. The mechanism includes 7 irreversible steps and 4 rapidly equilibrated protonation-deprotonation reactions

$$BrO_3^- + HSO_3^- \xrightarrow{k_1} H^+ + BrO_2^- + SO_4^{2-} \quad \text{(R1)}$$

$$BrO_2^- + 2HSO_3^- \xrightarrow{k_2} 2H^+ + 2SO_4^{2-} + Br^- \quad \text{(R2)}$$

$$BrO_2^- + 2H_2SO_3 \xrightarrow{k_3} 4H^+ + 2SO_4^{2-} + Br^- \quad \text{(R3)}$$

$$BrO_3^- + H_2SO_3 \xrightarrow{k_4} 2H^+ + BrO_2^- + SO_4^{2-} \quad \text{(R4)}$$

$$BrO_3^- + 2HFe(CN)_6^{3-} \xrightarrow{k_5} BrO_2^- + 2Fe(CN)_6^{3-} + H_2O \quad \text{(R5)}$$

$$BrO_2^- + 4HFe(CN)_6^{3-} \xrightarrow{k_6} Br^- + 4\,Fe(CN)_6^{3-} + 2H_2O \quad \text{(R6)}$$

$$BrO_2^- + 4Fe(CN)_6^{4-} + 4\,H^+ \xrightarrow{k_6} Br^- + 4Fe(CN)_6^{3-} + 2H_2O \quad \text{(R7)}$$

$$HSO_3^- \overset{K_1}{\rightleftharpoons} H^+ + SO_3^{2-} \quad \text{(E1)}$$

$$HFe(CN)_6^{3-} \overset{K_2}{\rightleftharpoons} H^+ + Fe(CN)_6^{4-} \quad \text{(E2)}$$

$$H_2SO_3 \overset{K_3}{\rightleftharpoons} H^+ + HSO_3^- \quad \text{(E3)}$$

$$HSO_4^- \overset{K_4}{\rightleftharpoons} H^+ + SO_4^{2-} \quad \text{(E4)}$$

As described in detail in our previous work,[7] based on this mechanism, a mathematical model can be formulated by writing mass balance equations involving all 13 chemical species. Assuming quasi-equilibrium states for the protonation-deprotonation reactions and a quasi-steady state for the intermediate $BrO_2^-$, we obtain an 8-variable model. Furthermore, a mass conservation constraint can be applied to each of the chemical elements taking part in the reacting species (sulfur, hydrogen, oxygen, bromine, and iron) as well as a charge conservation constraint. These six constraints allow for final reduction to two mass balance equations for the two species $H^+$ and $HSO_3^-$:

$$\frac{dH}{dt} = r_H + \Delta r_H + k_0(H_0 - H) \quad (1)$$

$$\frac{dHX}{dt} = r_{HX} + \Delta r_{HX} + k_0(HX_0 - HX) \quad (2)$$

where $H = [H^+]$, $HX = [HSO_3^-]$; $r_H$, $r_{HX}$ are net rates associated with the irreversible reactions R1−R7 and $\Delta r_H$, $\Delta r_{HX}$ are contributions from the rapidly established equilibria E1−E4. We have done test calculations with both the 8-variable and 2-variable models and found virtually no difference between both models, which implies that the simplifying assumptions hold. The inflow concentrations $H_0$ and $HX_0$ are calculated as concentrations of $H^+$ and $HSO_3^-$ in a hypothetical feed, where the relevant equilibrium (E1) is established, which implies

$$H_0 = 2K_1h_0/(s_0 - 2h_0),\ HX_0 = 2h_0 \quad (3)$$

where $s_0$ and $h_0$ are concentrations of $Na_2SO_3$ and $H_2SO_4$ in the feed, respectively.

To account for pulsed perturbations by $H^+$, $OH^-$, or $SO_3^{2-}$, an instantaneous equilibration of the reactions E1−E4 is assumed whereby both $H$ and $HX$ are instantaneously affected. Therefore, a relation between the instantaneous concentrations $H_I$ and $HX_I$ prior to the pulse and $H_{II}$ and $HX_{II}$ after the pulse is needed. Such a relation is obtained by considering the mass conservation constraints and electroneutrality condition equation.[7] For a perturbation $\Delta c_H$, $\Delta c_{OH}$, $\Delta c_X$ by acid, base or sulfite, respectively, we have

$$b_0 - 2h_0 - \Delta c_H + \Delta c_{OH} - 2\Delta c_X + H_{II} - K_V/H_{II} + HX_{II}(1 + 2H_{II}/K_2) + HS_{II} - B_{II} = 0 \quad (4)$$

with

$$HX_{II} = HX_I\frac{1 + K_1/H_I + H_I/K_2 + \Delta c_X}{1 + K_1/H_{II} + H_{II}/K_2},$$

$$B_{II} = B_I\frac{H_I + K_3}{H_{II} + K_3},\ HS_{II} = S_I\frac{1 + H_I/K_4}{1 + K_4/H_{II}}$$

where $K_v$ is the ionic product of water, $B = [Fe(CN)_6^{4-}]$, $S = [SO_4^{2-}]$, $HS = [HSO_4^-]$. Since we assume perturbation by one perturbant at a time, only one of the three $\Delta c$ terms is nonzero in a particular case. Equation 4 can be solved for $H_{II}$ provided that the composition immediately before the pulse is known.

### 4. Experimental Results

The main purpose of the experiments was to compare dynamics of the oscillatory and excitable system under periodic

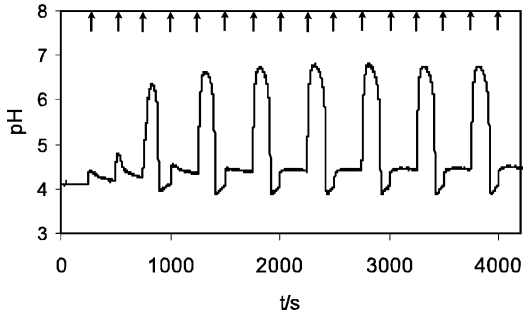


**Figure 1.** pH trace of the dynamical response to periodic perturbations of SSA by $OH^-$; $T = 250$ s, $\Delta c(OH^-) = 0.53$ mM, $k_0 = 8.0 \times 10^{-4}$ $s^{-1}$.

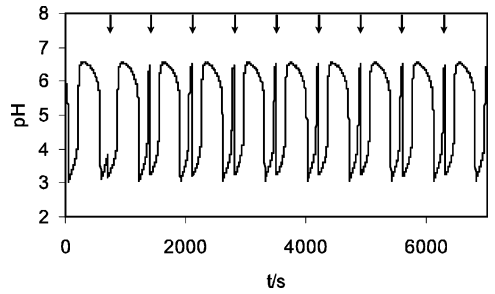


**Figure 2.** pH trace of the dynamical response to periodic perturbations of regular oscillations by $H^+$; $T = 700$ s, $\Delta c(H^+) = 3.54$ mM, $k_0 = 2.0 \times 10^{-3}$ $s^{-1}$.

forcing. We measured time series of pH representing the response of the system in two regions of different excitable dynamical modes and in the region of oscillatory dynamics. The acidic excitable steady state is sensitive to perturbations by a base, and consequently, we used NaOH and $Na_2SO_3$ as perturbants. We call this kind of excitability *inhibitory*[6] since the addition of base initiates an inhibitory process that raises pH before the activatory process of autocatalytic production of $H^+$ prevails and pH drops suddenly. The weakly acidic steady state is also excitable but pulses of $H_2SO_4$ are needed to elicit an excitatory response; we call this dynamical mode an *activatory* excitability whereby the activatory process is started directly by adding acid and causes pH to drop almost instantaneously. Periodic oscillations occur for $k_0$ between the two regions of excitability and we used both base (NaOH) and acid ($H_2SO_4$) as perturbants.

In the experiments with all of these perturbants, we systematically varied amplitude $\Delta c$ and period $T$ of perturbations, and we monitored the pH in the system. Examples of pH traces are shown in Figure 1, which represent dynamical responses in the case of the acidic stationary state SSA perturbed by pulsed addition of NaOH with the amplitude $\Delta c(OH^-) = 0.53$ mM and period $T = 250$ s. The response is a sequence of large-amplitude peaks or firings, corresponding to successful excitations. In this pattern, every other pulse gives rise to an excitation, and thus, the dynamics is locked with the external pulse sequence. Figure 2 displays dynamical response in the case of periodic oscillations (autonomous period $T_B = 520$ s) perturbed by addition of $H_2SO_4$ with the amplitude $\Delta c(H^+) = 3.54$ mM and period $T = 700$ s. Here the pattern is also locked with the external periodic input in a 1/2 ratio; the waveform of the broad peaks is essentially identical with that for autonomous oscillations, whereas the narrow peaks are attempted oscillations cut off by the pulsed addition of the acid. Finally, Figure 3 shows periodic pertubations of the weakly acidic steady-state SSB with the amplitude $\Delta c(H^+) = 4.96$ mM and period $T = 500$ s. In this case, the system is phase locked in a complex, higher order

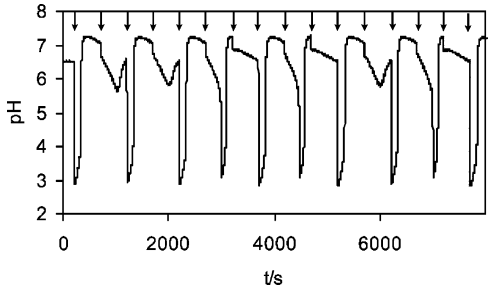


**Figure 3.** pH trace of the dynamical response to periodic perturbations of SSB by $H^+$; $T = 500$ s, $\Delta c(H^+) = 4.96$ mM, $k_0 = 3.6 \times 10^{-3}$ $s^{-1}$.

periodic pattern with 5 large-amplitude responses (sharp troughs of sudden decrease in *pH*) within an interval spanning 8 pulsed additions. Notice that this pattern is quickly established after a short initial transient.

**Firing Number.** Frequency locking (or resonance) can be conveniently described by introducing a firing number. Dynamical response has the form of a sequence of repeated oscillations/excitations. Both the oscillatory and excitatory dynamical modes can be described by counting the number of oscillations/excitations during the experimental run and calculating an average number of such firings per one forcing period. Only those oscillatory waveforms are counted which are fully completed before the next pulse is applied. Thus, the firing numbers for the excitatory and oscillatory regimes are

$$\nu_E = n_E/n_p \text{ or } \nu_O = n_O/n_p \tag{5}$$

where $n_E$ or $n_O$ is the number of excitatory or oscillatory responses, respectively, in a time interval given by the duration of the experimental run, and $n_P$ is the number of perturbations in the same time interval. In the excitatory regime, the system can fire only when perturbed, whereas in the oscillatory regime, the firings are actively produced and pulses can only quench or delay some of them. Therefore, $\nu_E$ can never be larger than 1 unlike $\nu_O$, which can attain any value. Pulsed perturbations are characterized by two parameters: $T$, the period of perturbations (time interval between two subsequent perturbations), and $\Delta c$(P), the amplitude of perturbation (moles of added perturbant P per volume of the reactor). If the response is periodic with a period $qT$, then the firing number is $\nu = p/q$ and $p$ is the number of firings within the period $qT$. We use $\nu$ for characterization of the dynamics at various values of $T$ and $\Delta c$(P). When a parameter is varied, a periodic regime with $\nu = p/q$ will generally exist within a certain range, and therefore, dependence of $\nu$ on a parameter is expected to be a stepwise varying function as the system switches from one resonance to another. The value of $\nu < 1$ corresponds to a subharmonic entrainment, $\nu = 1$ represents synchronized firing, and $\nu > 1$ is referred to as superharmonic entrainment.

Theoretic framework for the dependence of $\nu$ on $T$ for oscillatory systems under small-amplitude forcing is provided by a nondecreasing continuous piecewise constant function called a devil's staircase.[16] This kind of dynamics occurs in a wide variety of physical, chemical, and biological systems, e.g., see refs 17−21. Every plateau of the devil's staircase function corresponds to a $p/q$-periodic regime, and points at which $\nu$ is irrational correspond to quasiperiodicity. As the forcing amplitude increases, the quasiperiodicity vanishes as the measure of the set of $T$'s where $\nu$ is quasiperiodic shrinks to zero. Instead, chaotic dynamics appear, and the uniqueness and monotonicity of the devil's staircase break down.[22,23] A similar scenario holds for perturbed excitable systems, except for that quasiperiodicity

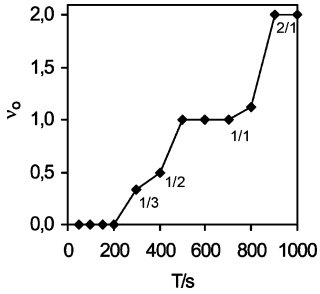


**Figure 4.** Dependence of firing number on the period of forcing for the oscillatory regime (autonomous period $T_B = 520$ s) perturbed by $OH^-$; $\Delta c(OH^-) = 2.48$ mM, $k_0 = 2.0 \times 10^{-3}$ s$^{-1}$.

may be absent.[24] Naturally, subtle structure of transitions according to this theoretical framework cannot be directly compared with experimentally measured $\nu$ because of finite time measurements and the presence of noise. Nevertheless, $\nu$ is a convenient measure for comparing measurements with calculations so as to test the mechanism and model that we developed in previous work.[7]

**Firing Diagrams.** For a typical experiment, the forcing amplitude $\Delta c$(P) was set, the forcing period $T$ was sequentially varied, and the firing number was calculated from the recorded pH trace for each value of $T$. For example, the dependence of the firing number $\nu_O$ of an oscillatory regime forced by adding $OH^-$ on $T$ for a given amplitude is plotted in Figure 4. As expected, the graph is displaying the stairlike structure, and the firing number spans an interval from 0/1- to 2/1-phase locking. By running experiments at different values of $\Delta c$(P), two-parameter firing diagrams are obtained by combining all of the "staircases" with different perturbation amplitudes. These 3D plots globally represent the response dynamics as shown in Figure 5a−e.

The firing number as a function of $\Delta c$ and $T$ for the weakly acidic steady state SSB periodically perturbed by acid is shown in Figure 5a. The fully synchronized responses ($\nu_E = 1/1$) are obtained either for a sufficiently large period or for a sufficiently large amplitude, giving the corresponding plateau a triangular shape. There is also a sizable domain of intermediate firing numbers with values around 1/2 where the staircase in both parameter directions is gradual. Interestingly, the firing rate for small $T$ and medium $\Delta c$ is higher than that for nearby higher values of $T$, and therefore the surface of firing numbers in the subharmonic region ($\nu_E < 1$) has a saddle shape. Figure 5b,c displays firing behavior of acidic steady-state SSA. The response to perturbations by a base, Figure 5b, differs from that by a sulfite, Figure 5c, in several aspects. First, the staircase is rather gradual in the former, whereas it is steep in the latter. This feature appears in the direction of both $\Delta c$ and $T$, giving the plateau of 1/1-regime triangular (Figure 5b) and rectangular (Figure 5c) shapes. Second, the threshold amplitude $\Delta c(OH^-)$ for excitations to occur is smaller by 1 order of magnitude than that for $\Delta c(SO_3^{2-})$. Clearly, both $OH^-$ and $SO_3^{2-}$ consume $H^+$ and thereby lower its concentration below the threshold, but a larger amount of $SO_3^{2-}$ is necessary to invoke an excitation. Third, there is a distinct plateau at the 1/2-regime and a hint of a plateau at the 1/3-regime in Figure 5b, whereas Figure 5c does not show any significant plateau except for the 1/1-regime.

Parts d and e of Figure 5 correspond to pulsed forcing of oscillatory regime by acid and base, respectively. The range of the firing number $\nu_O$ here is from 0 to 2 which corresponds to the perturbation period up to twice that of the autonomous oscillations (with period $T_B = 520$). The system tends to frequency-locked regimes much more readily when perturbation by acid is used, in particular, 0/1, 1/1, and 2/1 regimes are dominant in Figure 5d, especially for larger $\Delta c(H^+)$. On the other hand, when the base is used as perturbant, the staircase

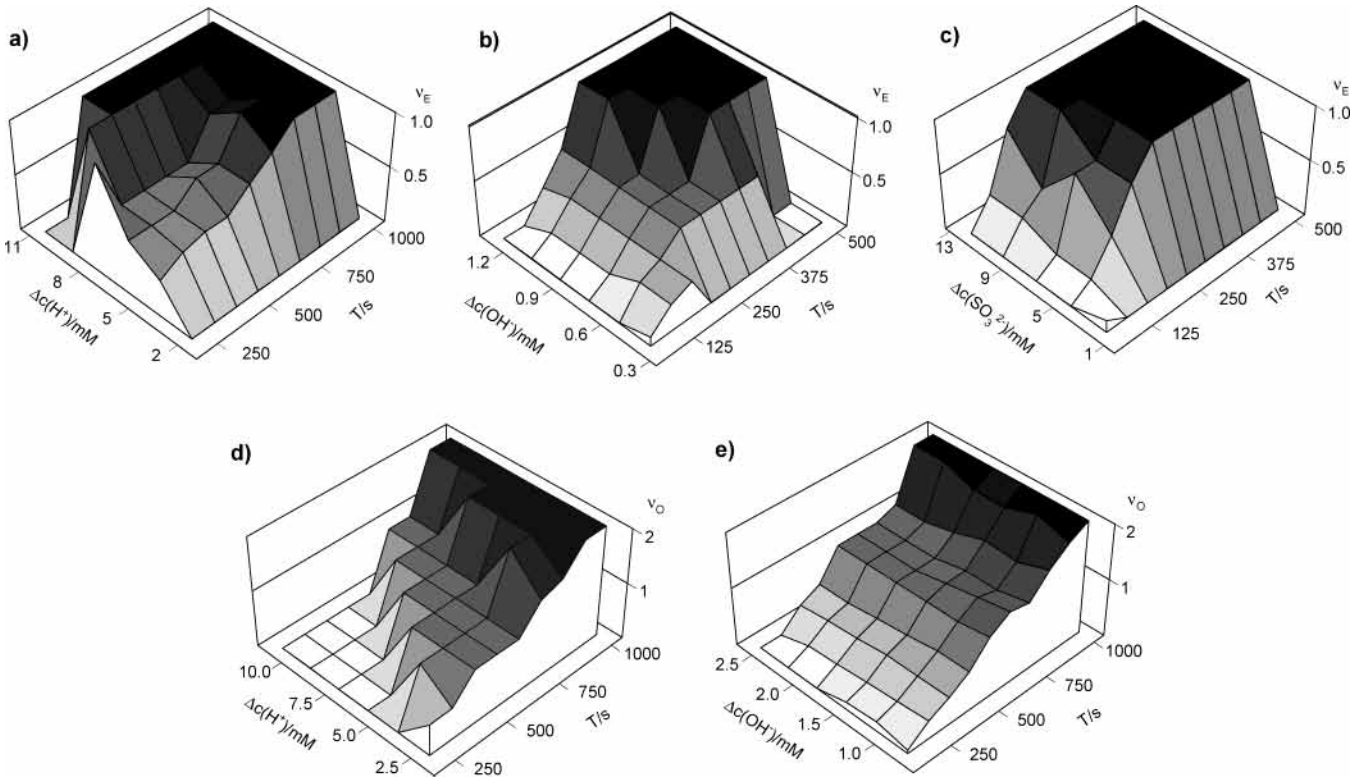


**Figure 5.** Experimentally measured two-parameter dependence of firing number on period and amplitude of forcing. (a) SSB perturbed by $H^+$, $k_0 = 3.6 \times 10^{-3}$ s$^{-1}$, (b) SSA perturbed by $OH^-$, $k_0 = 8.0 \times 10^{-4}$ s$^{-1}$, (c) SSA perturbed by $SO_3^{2-}$, $k_0 = 8.0 \times 10^{-4}$ s$^{-1}$, (d) oscillations perturbed by $H^+$, $k_0 = 2.0 \times 10^{-3}$ s$^{-1}$, (e) oscillations perturbed by $OH^-$, $k_0 = 2.0 \times 10^{-3}$ s$^{-1}$.

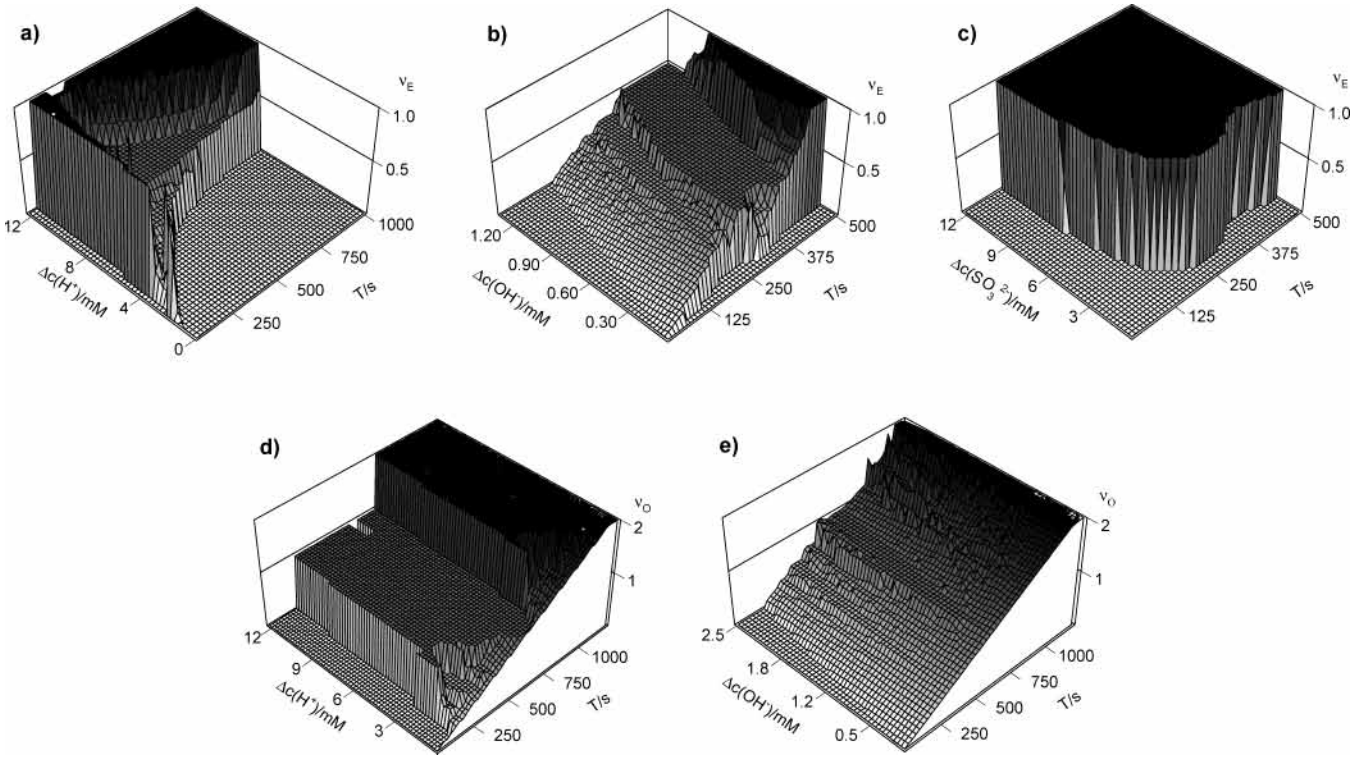


**Figure 6.** Numerically calculated two-parameter dependence of firing number on period and amplitude of forcing. (a) SSB perturbed by $H^+$, $k_0 = 6.0 \times 10^{-3}$ s$^{-1}$, (b) SSA perturbed by $OH^-$, $k_0 = 8.0 \times 10^{-4}$ s$^{-1}$, (c) SSA perturbed by $SO_3^{2-}$, $k_0 = 8.0 \times 10^{-4}$ s$^{-1}$, (d) oscillations perturbed by $H^+$, $k_0 = 2.0 \times 10^{-3}$ s$^{-1}$, (e) oscillations perturbed by $OH^-$, $k_0 = 2.0 \times 10^{-3}$ s$^{-1}$.

in the direction of $T$ is rather gradual in Figure 5e so that no frequency locking is dominant, even though 1/1 and 2/1 regimes form small plateaus. A marked difference between the two perturbants is that the increase of $\Delta c(OH^-)$ does not cause any significant effect, whereas the perturbation by acid causes a decrease in the $\Delta c(H^+)$ direction.

## 5. Calculated Results

Calculations were done by using the LSODE package for solving a system of ordinary differential equations.[25] At each set of parameter values, a run over sufficiently long time interval was performed and firings were counted. For that, we need to distinguish between a response representing and excitation and that which does not. This could be done empirically by inspection of the time series, as it was done in experiments. However, we can do better by considering the structure of trajectories in the phase plane and finding a threshold set for excitations. For excitability with multiple steady states (one of them stable and excitable), the threshold set is simply a stable separatrix of the saddle. Since both SSA and SSB are unique steady states under conditions corresponding to measurements, the threshold set cannot be formed by stable separatrices. Instead, we used a method of calculating the threshold set that we developed earlier.[6,13] The calculated threshold is a piece of trajectory in the phase plane of eqs 1 and 2 that has certain marginal stability properties and provides a natural boundary between large-loop and small-loop trajectories. A pulse penetrating this set was considered as corresponding to an excitatory response. The threshold set exists even in the case of oscillatory autonomous dynamics and so the calculation of firing number was done analogously.

**Firing Diagrams.** Figure 6a−e comprises the dependence of the firing number on $T$ and $\Delta c$(P) calculated from the two-variable model according to eqs 1 and 2 and correspond to parts a−e of Figure 5 obtained from experiments. Response dynamics to perturbation of the weakly acidic steady-state SSB by acid is shown in Figure 6a. The dominant plateaus correspond to 0/1, 1/2 and 1/1 lockings but a distinct finer staircase structure is observed in the transition zones between these plateaus in both $T$ and $\Delta c$ directions. There are two regions of the 1/1-regime. The larger one is triangular as in the experiments, and the smaller one forms a narrow stripe extending in the $\Delta c$ direction for small values of $T$. In parts b and c of Figure 6, the acidic steady-state SSA is perturbed by adding sodium hydroxide and sodium sulfite, respectively. The first case corresponds to a gradual stepwise increase of the firing number in the $T$ direction with many plateaus of frequency locked regimes. In the direction of $\Delta c(OH^-)$, there is a sudden jump from the 0/1 regime corresponding to subthreshold amplitudes to a particular regime for a given $T$ with nonzero $\nu_E$, which then remains essentially unchanged as the amplitude is increased further on. The plateaus of 0/1, 1/2, and 1/1 are the largest, but other frequency-locked regimes, particularly those with $\nu_E = 1/n$, $n > 2$, are present. In contrast, perturbation by sulfite in Figure 6c shows only 0/1 and 1/1 locking. For small amplitudes, the system is perturbed by subthreshold perturbations and does not respond by excitations for any periods of forcing; likewise for small enough periods, there is no firing for any amplitude. The plateau of the 1/1 regime is large and square-shaped.

Firing behavior of the periodically forced oscillatory regime is shown in Figure 6d,e. Perturbation by acid (Figure 6d) generates very distinct steps in the $T$ direction associated with large plateaus of 0/1, 1/1, and 2/1 regimes. Only for quite small forcing amplitudes the staircase possesses a subtle structure involving numerous resonances. The main plateaus broaden very sharply with increasing $\Delta c(H^+)$ and then maintain a constant width so that the firing number is almost independent of the forcing amplitude. On the other hand, perturbation by base

(Figure 6e) causes a gradual stepwise increase of $\nu_O$ with $T$ with many plateaus of various frequency-locked regimes. Occasionally, the staircase decreases locally, which indicates a complex chaotic dynamical behavior.[23] There is little variation of $\nu_O$ with $\Delta c(OH^-)$ as in the previous case.

## 6. Discussion and Conclusions

Experimental two-parameter firing diagrams in Figure 5 show that the system under periodic forcing becomes entrained with the external forcing at various subharmonic periodic regimes if the autonomous dynamics is excitable and both sub- and superharmonic regimes if the autonomous dynamics is oscillatory. The frequency-locked regimes are indicated by the firing number in the form $p/q$ where $p$ is the number of firings and $q$ is the number of pulses such that the dynamical patterns repeat itself after a period $qT$. The dominant resonances are 0/1,1/2, and 1/1 for excitatory responses and, in addition, 2/1 for oscillatory responses. Apart from those, there exist higher order resonances as well as nonperiodic responses. The staircase in the $T$ direction is typically nondecreasing which reflects an enhanced ability of the system to respond by a firing if the forcing period is increased. For excitable dynamics, this is implied by a longer relaxation time during which the system can recover its excitability. For oscillatory dynamics, the system can simply generate more spontaneous oscillations between two consecutive pulses if $T$ is increased.

We can test the ability of the model to reproduce the experimental measurements by comparing corresponding graphs in Figures 5a−e and 6a−e. Experiments and calculations in the case of perturbation of SSA by sulfuric acid (Figures 5a and 6a) share an interesting feature: a local drop of firing number when $T$ is varied. The measured firing rate at low forcing periods is high ($\nu_E = 1$ at some points) then drops to a value near to 1/2 and again raises to 1 as $T$ is increased. Exactly the same behavior is found in the calculations. The dependence of $\nu_E$ on $\Delta c(H^+)$ is either monotonic (calculations) or with a shallow minimum (experiments) leading to a saddle-shaped surface in both cases. Experiments and calculations for perturbation by sodium hydroxide (Figures 5b and 6b) correspond well in showing a gradual stepwise increase of the firing number in the direction of the forcing period $T$. The domain of the 1/2 regime is smaller in experiments and does not extend for large $\Delta c$. At the same time, the domain of the 1/1 regime is larger in experiments at the expense of the 1/2 regime. Apart from this discrepancy, the overall picture is in mutual agreement. Perturbation of the acidic steady state SSA by sulfite leads in both cases to a large, more or less rectangular region of the 1/1 resonance. The experiments (Figure 5c) show a domain of subharmonic regimes, whereas calculations (Figure 6c) predict only a 0/1 or 1/1 resonance. Despite this, the correspondence of the 1/1 regime in both cases is quite satisfactory. The oscillatory regime perturbed by acid (Figures 5d and 6d) displays dominant regions of 0/1, 1/1, and 2/1 resonances in both experiments and calculations, only the domains are triangular in the experiments but rectangular in the calculations. Finally, correspondence in the case of perturbation by base (Figures 5e and 6e) is very close; the dependence of the firing number on $T$ is gradual, whereas the dependence on $\Delta c$ is weak in both experiments and calculations. There is an additional fine structure in the calculated results displayed as local dents in Figure 6e, signifying that the staircase is nonmonotonic in the $T$ direction. Such a behavior indicates the presence of chaotic dynamics.[23] Notice that the flow rates correspond exactly to experimental values in the case of SSA and the oscillatory regime, whereas for SSB, the numerical value of the flow rate ($k_0 = 6.0 \times 10^{-3}\ s^{-1}$) is larger than that for the experiments ($k_0 = 3.6 \times 10^{-3}\ s^{-1}$). This discrepancy was discussed in ref 7 and can be probably attributed to a reaction pathway involving ferricyanide, which is not included in the presented mechanism. Based on work in ref 7, the numerical value of $k_0$ was set so that the threshold value of $\Delta c$ for obtaining an excitation was the same as in experiments.

The model seems to reflect the response dynamics rather well; the ranges of amplitudes and forcing periods are closely matching experiments, and in many cases, the structure of the staircase is also in good agreement. We have shown earlier that the model reproduces a bifurcation diagram in the absence of perturbations[6] as well as more subtle features, such as the thresholds of excitability.[7] Our results provide further experimental evidence in support of the model. Good predictability of dynamics under periodic pulsed perturbations implies that the threshold phenomena are also well reflected by the model.

The firing diagrams show that the structure of the frequency locked regions is dependent on the perturbant. Thus, it is possible to analyze the role which a particular perturbant plays in the mechanism.[26] Although addition of $OH^-$ supports many different frequency locked regimes, as expressed by gradual staircase in $T$ direction, addition of $H^+$ causes the system to prefer one of the major resonances: 0/1, 1/2, or 1/1 for perturbed excitable steady state and, in addition, 2/1 for perturbed periodic oscillations. Addition of sulfite leads to the 0/1 or 1/1 regime, and the 1/2 resonance is entirely suppressed. These differences may reflect the respective roles: $H^+$ is the autocatalytic species, $OH^-$ directly inhibits the autocatalysis, and $SO_3^{2-}$ inhibits the autocatalysis but simultaneously gives rise to $HSO_3^-$ which provides a negative feedback loop required for nonlinear dynamics such as excitability and oscillations. It would be interesting to systematically examine other nonlinear chemical systems by exposing them to pulsed perturbations and compare the firing diagrams with the present results to verify whether the suggested differences in their structure can be generalized. In this regard, the work reported here is a first step toward this goal.

**Acknowledgment.** This work has been supported by grants from the Czech Science Foundation No. GA203/03/0488 and a project from the Czech Ministry of Education No. MSM2234-00007.

## References and Notes

(1) Kosek, J.; Marek, M. *J. Phys. Chem.* **1993**, *97*, 120.

(2) Nevoral, V.; Votrubová, V.; Hasal, P.; Schreiberová, L.; Marek, M. *J. Phys. Chem. A* **1997**, *101*, 4954.

(3) Votrubová, V.; Hasal, P.; Schreiberová, L.; Marek, M. *J. Phys. Chem. A* **1998**, *102*, 1318.

(4) Hohmann, W.; Kraus, M.; Schneider, F. W. *J. Phys. Chem. A* **1997**, *101*, 7364.

(5) Hohmann, W.; Kraus, M.; Schneider, F. W. *J. Phys. Chem. A* **1998**, *102*, 3103.

(6) Zagora, J.; Voslař, M.; Schreiberová, L.; Schreiber, I. *Faraday Discuss.* **2001**, *120*, 313.

(7) Zagora, J.; Voslař, M.; Schreiberová, L.; Schreiber, I. *Phys. Chem. Chem. Phys.* **2002**, *4*, 1284.

(8) Orbán, M.; Epstein, I. R. *J. Am. Soc.* **1987**, *109*, 101.

(9) Orbán M.; Kurin-Csörgei, K.; Zhabotinsky, A. M.; Epstein, I. R. *Faraday Discuss.* **2001**, *120*, 11.

(10) Edblom, E. C.; Luo, Y.; Orbán, M.; Kustin, K.; Epstein, I. R. *J. Phys. Chem.* **1989**, *93*, 2722.

(11) Rábai, G.; Kaminaga, A.; Hanazaki, I. *J. Phys. Chem.* **1996**, *100*, 16441.

(12) Boissonade, J.; De Kepper, P. *J. Phys. Chem.* **1980**, *84*, 501; De Kepper, P. Boissonade, J. *J. Chem. Phys.* **1981**, *75*, 189.

(13) Guckenheimer, J. *Physica* **1986**, *20D*, 1.
(14) Nevoral, V.; Voslař, M.; Schreiber, I.; Hasal, P.; Marek, M. *Forma* **2000**, *15*, 291.
(15) Williamson, F. S.; King, E. L. *J. Am. Chem. Soc*. **1957**, *79*, 5397.
(16) Bak, P. *Physics Today* **1986**, December, 38; Bak, P. *Rep. Prog. Phys.* **1982**, *45*, 587.
(17) Parlitz, U.; Lauterborn, W. *Phys. Rev. A* **1987**, *36*, 1428.
(18) Sen, A. K. *Int. J. Bifurcat. Chaos* **2001**, *11*, 583.
(19) Brons, M.; Gross, P.; Bar-Eli, K. *Int. J. Bifurcat. Chaos* **1997**, *7*, 2621.
(20) De Brouwer, S.; Edwards, D. H.; Griffith, T. M. *Am. J. Physiol.-Heart. C* **1998**, *43*, H1315.
(21) Havsteen, B. *J. Theor. Biol*. **1997**, *189*, 367.
(22) Boyland, P. L. *Commun. Math. Phys*. **1986**, *106*, 353.
(23) Hockett, K.; Holmes, P. *P. Am. Math. Soc.* **1988**, *102*, 1031.
(24) Ringland, J.; Issa, N.; Schell, M. *Phys. Rev. A* **1990**, *41*, 4223.
(25) Hindmarsh, A. C. In *Scientific Computing*; Stepleman, R. S., et al., Eds.; North-Holland: Amsterdam, 1983; pp 55−64.
(26) Eiswirth, M.; Freund, A.; Ross, J. *Adv. Chem. Phys.* **1991**, *80*, 127.